POZNAN UNIVERSITY OF TECHNOLOGY ACADEMIC JOURNALS
No 91 Electrical Engineering 2017

DOI 10.21008/j.1897-0737.2017.91.0026

Mariusz BARAŃSKI*

FIELD-CIRCUIT ANALYSIS OF LSPMS MOTOR SUPPLIED WITH DISTORTED VOLTAGE

A line start permanent magnet synchronous motor (LSPMSM) supplied with distorted voltage is analysed. The study is based on the field–circuit model. The algorithm for solving the equations of the model is discussed. In the analysis of the selected states of the motor the non–linearity of the magnetic circuit and skewed slots of the rotor are taken into consideration. In order to verify the developed algorithm and software, among others the startup process of the motor has been examined. The electromagnetic torque and phase currents are calculated. The results of computations have been compared to the results obtained using the commercial FEM package Comsol Multiphisics. Selected results of simulation tests are shown.

KEYWORDS: FE method, line start permanent magnet synchronous motor, distorted voltage, in–house software, Comsol package

1. INTRODUCTION

Induction motors still used in electric drives are being increasingly replaced by synchronous motors with permanent magnets (PMSM). This is due to the reduction of operating costs of the latter ones, resulting from the increase in the efficiency and power factor while reducing their dimensions in comparison with conventional induction motors of the same power. Many interesting PMSM constructions have been described in the literature. Motors with segmented magnets placed on the rotor surface are presented in papers [1, 2]. In order to reduce time and production costs, it is proposed e.g. to make motor components of powder material in one technological process [3, 4].

The main disadvantage of the PMSM is the necessity to make use of electronic power converter systems to make them start. This significantly increases the costs of the entire drive system. In order to avoid this drawback, intensive works on the LSPMSM are carried out in many scientific research centers over the world [5, 6].

* Poznan University of Technology.

2. EXAMINED MOTOR

The prototype of the designed LSPMS motor (Fig. 1) was examined. In the considered construction, the stator and frame of a 4 poles, Sg100L–4B type, 3 kW induction motor, were used. In the design process of new constructions of the LSPMSM, it is beneficial to utilize components of the classic asynchronous motor. The key reason is the manufacturing costs reduction, by keeping motor sizes and their interfaces in the range of produced series of induction machines.

a)

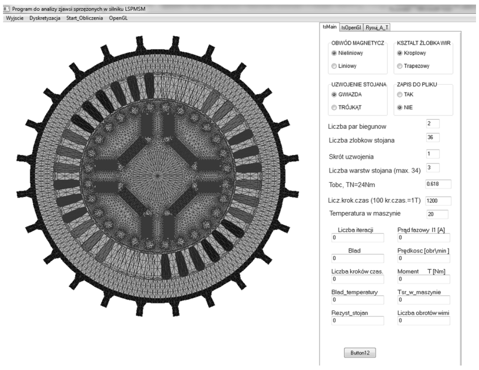

b)

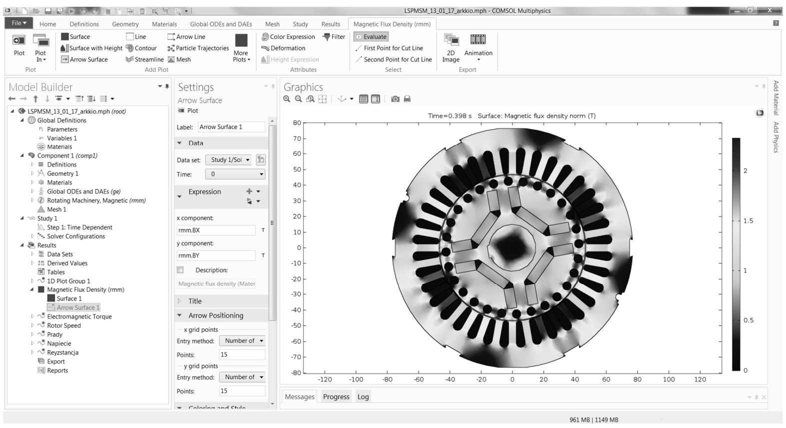

Fig. 1. The LSPMSM structures: in–house software (a) and COMSOL software package (b)

The rated line to line supply voltage of the base LSPMSM was equal to 400V (star connection). The stator consists of 36 slots and is wound with a single layer 3 phase windings. The rotor cage has 28 bars manufactured from aluminum (Fig. 1). In the rotor of the LSPMSM, the magnets are placed over a "U" arrangement of N38SH magnets embedded into the laminated rotor core (Fig. 1) [7].

3. FINITE ELEMENT FORMULATION

The 2D field distribution using magnetic vector potential $\boldsymbol{A}$, may be describe by equation (1)–(3).

$$\nabla \times \left(\frac{1}{\mu} \nabla \times \boldsymbol{A} \right) = \boldsymbol{J} + \boldsymbol{J}_m \tag{1}$$

$$\boldsymbol{J} = -\sigma \left(\mathrm{d}\boldsymbol{A}/\mathrm{dt} + \nabla \boldsymbol{V} \right) \tag{2}$$

$$\boldsymbol{J}_m = \nabla \times \boldsymbol{M} \tag{3}$$

where μ is the magnetic permeability, $\boldsymbol{J}$ is the current density vector, σ is the conductivity, $\boldsymbol{J}_m$ is the current density vector representing the magnetization of the permanent magnet, $\boldsymbol{M}$ is the magnetization vector in the region with permanent magnets.

In considerations, it has been assumed that the magnetic properties of magnetic soft materials and permanent magnets are described by equation (4) and (5) respectively [10].

$$\boldsymbol{B} = \mu(\boldsymbol{H}) \tag{4}$$

$$\boldsymbol{B} = \mu_0 (\boldsymbol{H} + \boldsymbol{M}) \tag{5}$$

where $\boldsymbol{B}$ is the vector of magnetic flux density, $\boldsymbol{H}$ is the magnetic field strength vector, μ_0 is the magnetic permeability of the vacuum.

Generally, when dealing with voltage–excited fields in devices containing non–linear elements, the current in windings is not known in advance. Therefore, one needs to take into consideration the electric circuit equations of these devices. The set of independent loop circuit equations may be written as follows

$$\boldsymbol{u} = \boldsymbol{R}\boldsymbol{i} + \frac{\mathrm{d}}{\mathrm{dt}} \boldsymbol{\Psi} \tag{6}$$

where $\boldsymbol{u}$ is the vector of supply voltage, $\boldsymbol{R}$ is the diagonal matrix of loop resistance, $\boldsymbol{i}$ is the loop current vector, $\boldsymbol{\Psi}$ is the vector of flux linkage with windings.

The equations of field–circuit model are coupled through the electromagnetic torque T to the equation of motion

$$J \frac{\mathrm{d}^2 \alpha}{\mathrm{d} t^2} + T_L + T_f = T \tag{7}$$

where J is the moment of inertia, α is the angular position of the rotor, T_L is the load torque, T_f is the resistive torque produced in the motor bearings and fan.

The electromagnetic torque T in equation (7) is calculated on the basis of the magnetic field distribution [9].

The space and time discretization method is used to solve non–linear equations (1)–(6) [8]. The method consists in searching for the value of the function describing the vector potential distribution in a set of discreet points. In the paper the finite element method is used, in which the magnetic circuit is divided into triangular elements. In time discretization the differential equations of the machine are substituted with algebraic equations describing field distribution and current propagation for subsequent time steps t_n, $n = 1, 2, 3\ldots$.

The set of the algebraic equations describing the electromagnetic field and the currents in the windings of the machine takes the following form

$$\begin{bmatrix} \boldsymbol{S}^n + \boldsymbol{G}\,(1-\boldsymbol{C}\,)\Delta t^{-1} & -\boldsymbol{z} \\ -\left[\boldsymbol{z}^T\right] & -\left(\boldsymbol{R}\Delta t + \boldsymbol{L}\right) \end{bmatrix} \begin{bmatrix} \boldsymbol{\varphi}^n \\ \boldsymbol{i}^n \end{bmatrix} = \begin{bmatrix} \mathbf{M}_m^n \\ -\Delta t \boldsymbol{U}^n \end{bmatrix} + \begin{bmatrix} \boldsymbol{G}\,(1-\boldsymbol{C}\,)\Delta t^{-1} & \mathbf{0} \\ -\boldsymbol{z}^T & -\boldsymbol{L} \end{bmatrix} \begin{bmatrix} \boldsymbol{\varphi}^{n-1} \\ \boldsymbol{i}^{n-1} \end{bmatrix} \tag{8}$$

where Δt is the time step length, $\boldsymbol{S}^n$, $\boldsymbol{G}$, $\boldsymbol{C}$, $\boldsymbol{z}$ are the coefficients submatrices, φ is the vector of the modified node potential, $\boldsymbol{M}_m$ is the vector of magnetomotive force in regions with the permanent magnets, $\boldsymbol{L}$ is the matrix of self–inductance and mutual inductance of end of windings. In the equation above the n index is used to show quantities for $t = t_n$ time steps and the n–1 index applies to quantities for $t = t_{n-1}$ time steps.

The movement of the rotor is simulated by means of the moving band method. In the elaborated algorithm and computer software equations (7) and (8) are solved with the aid of the Newton-Raphson iterative procedure. The electromagnetic torque was calculated using the FE representation of the Maxwell stress tensor formula (9) [10].

$$T = \nu_0\, l r_w^2 \int_0^{2\pi} \left(B_r B_\alpha\right)_{r=r_w} \mathrm{d}\alpha \tag{9}$$

where l is the core length of the motor, r_w is the radius of the surface where the electromagnetic torque is calculated, B_r and B_α is the magnetic flux density in the radial and tangential directions, respectively.

The formula was obtained by the analysis of the virtual displacement corresponding to the moving band method.

4. SIMULATED MODELS

On the basis of the presented algorithm an in–house software for the field analysis of LSPMS motor operation was developed. The in–house software makes it possible to analyse motor operation in transient states under variable load conditions and to simulate operation at distorted voltage–excited supply. In the paper the influence of harmonic content in the applied voltage on electromagnetic torque and phase current was tested. The results of computer simulations have been compared to the results obtained by using Comsol Multiphisics software.

Generally, electrical machines don't work with nominal load; they work with load approximately to 80%T_{LN}. The load of considered motor, adequately the torque equal to 80 per cent the nominal torque T_L=19.2 Nm, was considered. Calculations were carried out assuming that the magnetic circuit is non–linear. The analyses were performed for the motor supplied with 50Hz frequency voltage and with the distorted voltage with 5% and 10% content of the 5th and 7th harmonics respectively.

The distorted voltage curves are presented in Fig. 2. Analysing the curves of the electromagnetic torque and the phase currents for loaded motor obtained by using in–house software as well as commercial Comsol package are presented in Figs. 3 to 6.

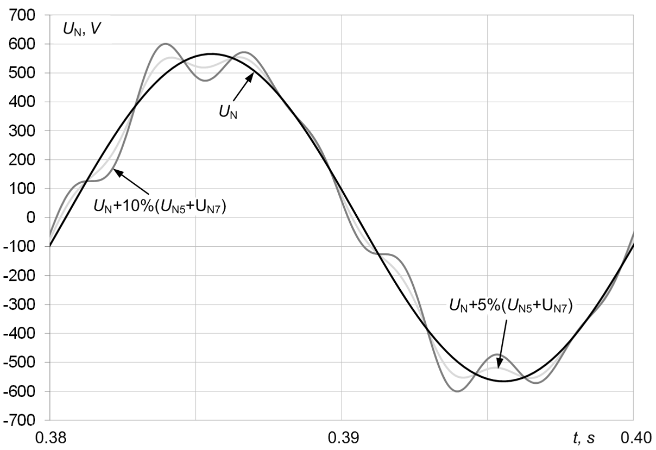

Fig. 2. Supply voltage time curves at 5% and 10% content of 5th and 7th harmonics

In table 1 has been summarized of *rms* value of phase currents and amplitudes of electromagnetic torque.

Table. 1. RMS phase currents and amplitude of electromagnetic torque

	in–house software			Comsol		
	U_N	U_N + +5% (U_{N5+} U_{N7})	U_N + +10% (U_{N5+} U_{N7})	U_N	U_N + +5% (U_{N5+} U_{N7})	U_N + +5% (U_{N5+} U_{N7})
I_{rms} [A]	6.12	6.51	7.19	6.87	7.60	8.45
T [Nm]	20.08	22.00	24.40	26.50	29.30	36.50

Analysing the electromagnetic torques and phases currents, we conclude that the amplitude of phases currents for 10 per cent content harmonics in in–house software increases by about 9.45 per cent than for amplitude of phases curves for 5 per cent content harmonics in supply voltage. However, the calculated electromagnetic torque is increases by above 9.83 per cent. The calculated phase current using Comsol is increases by about 10.01 per cent and the calculated electromagnetic torque is increasing by about 19.72 per cent. Moreover, analysing the high harmonics we can observe that significant contribution to the distorted voltage has 5th harmonic.

a)

b)

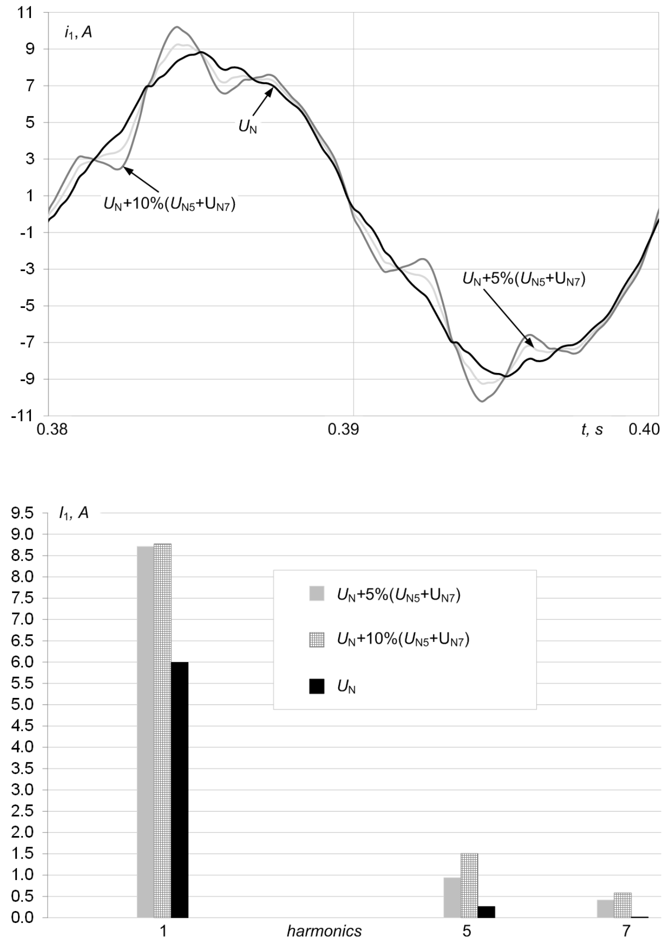

Fig. 3. Phase current at 5% and 10% content of 5th and 7th harmonics: time curves (a), high harmonics analysis (b) – in–house software

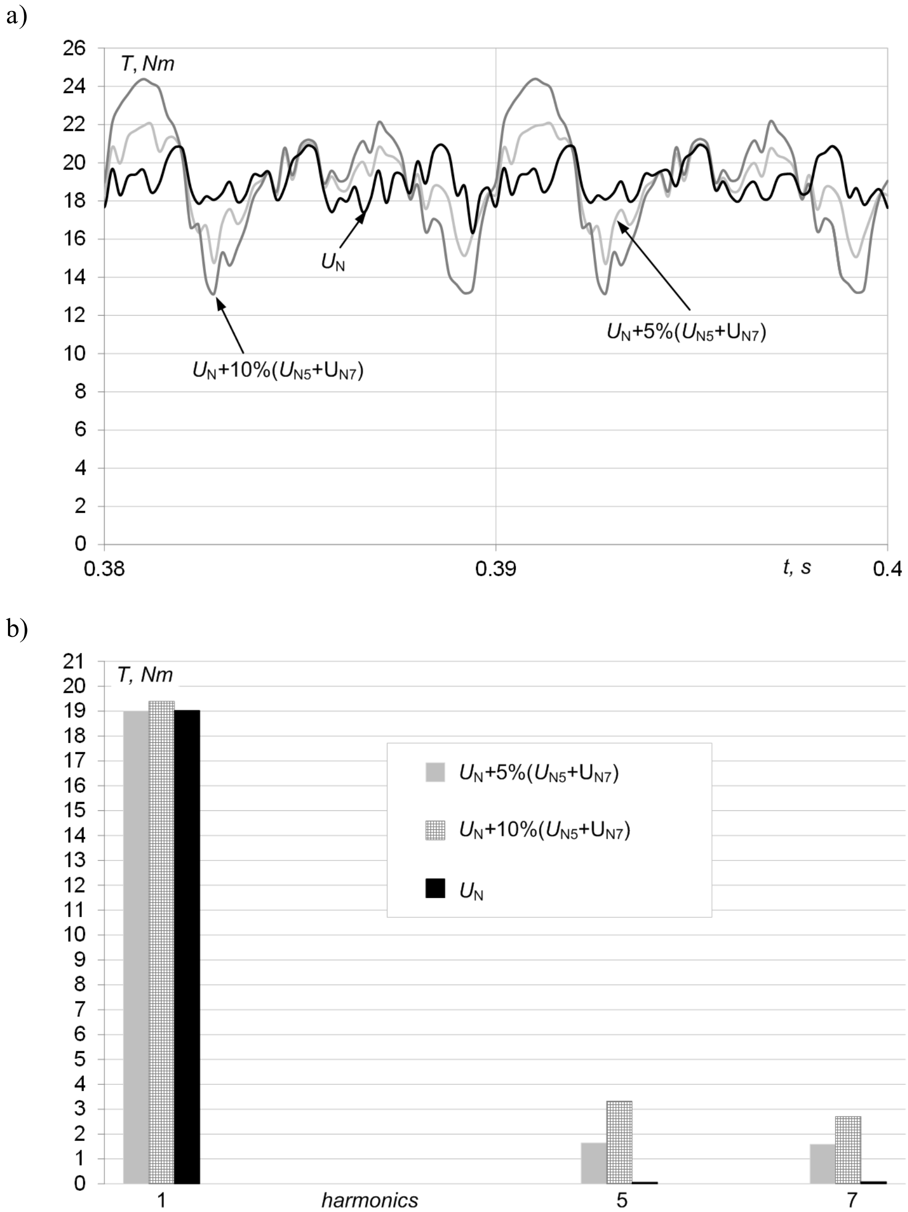

Fig. 4. Electromagnetic torque at 5% and 10% content of 5th and 7th harmonics: waveforms. (a). high harmonics analysis (b) – in–house software

a)

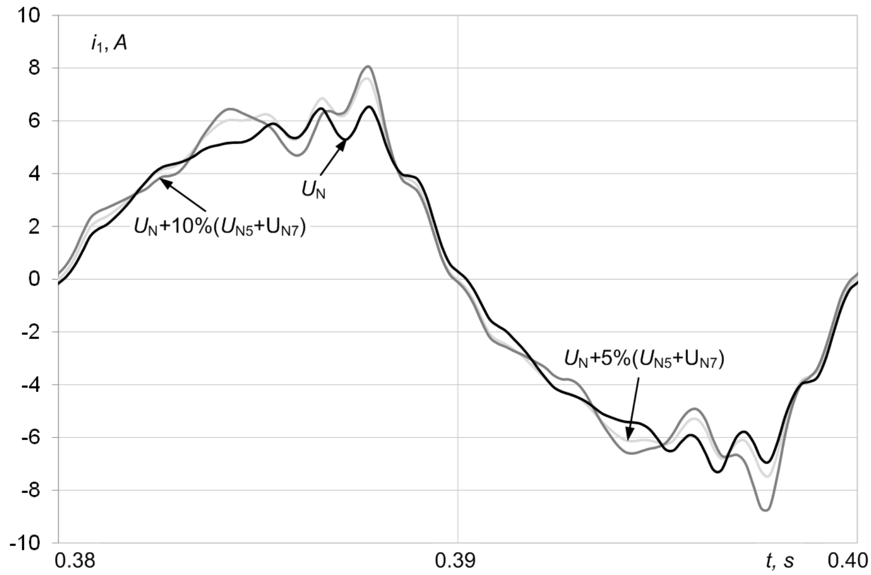

b)

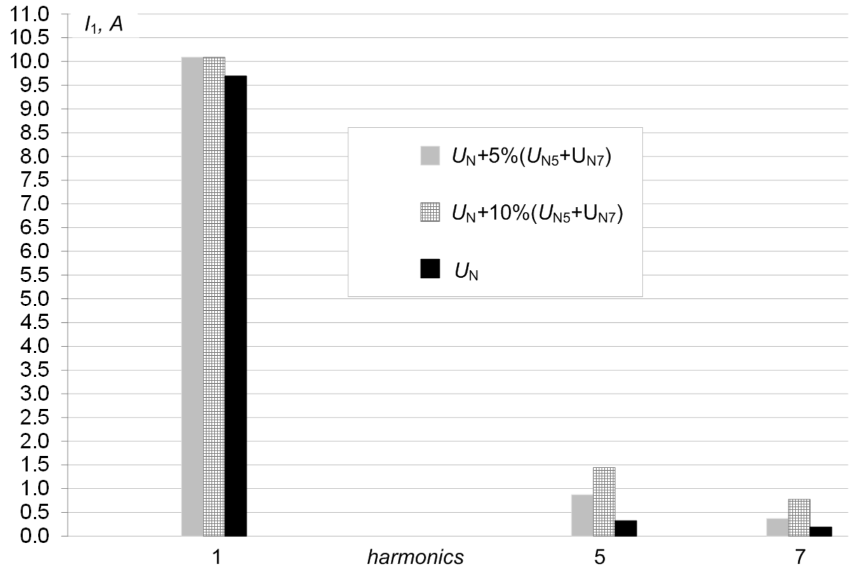

Fig. 5. Phase currents at 5% and 10% content of 5th and 7th harmonics: time curves (a), high harmonics analysis (b) – Comsol software

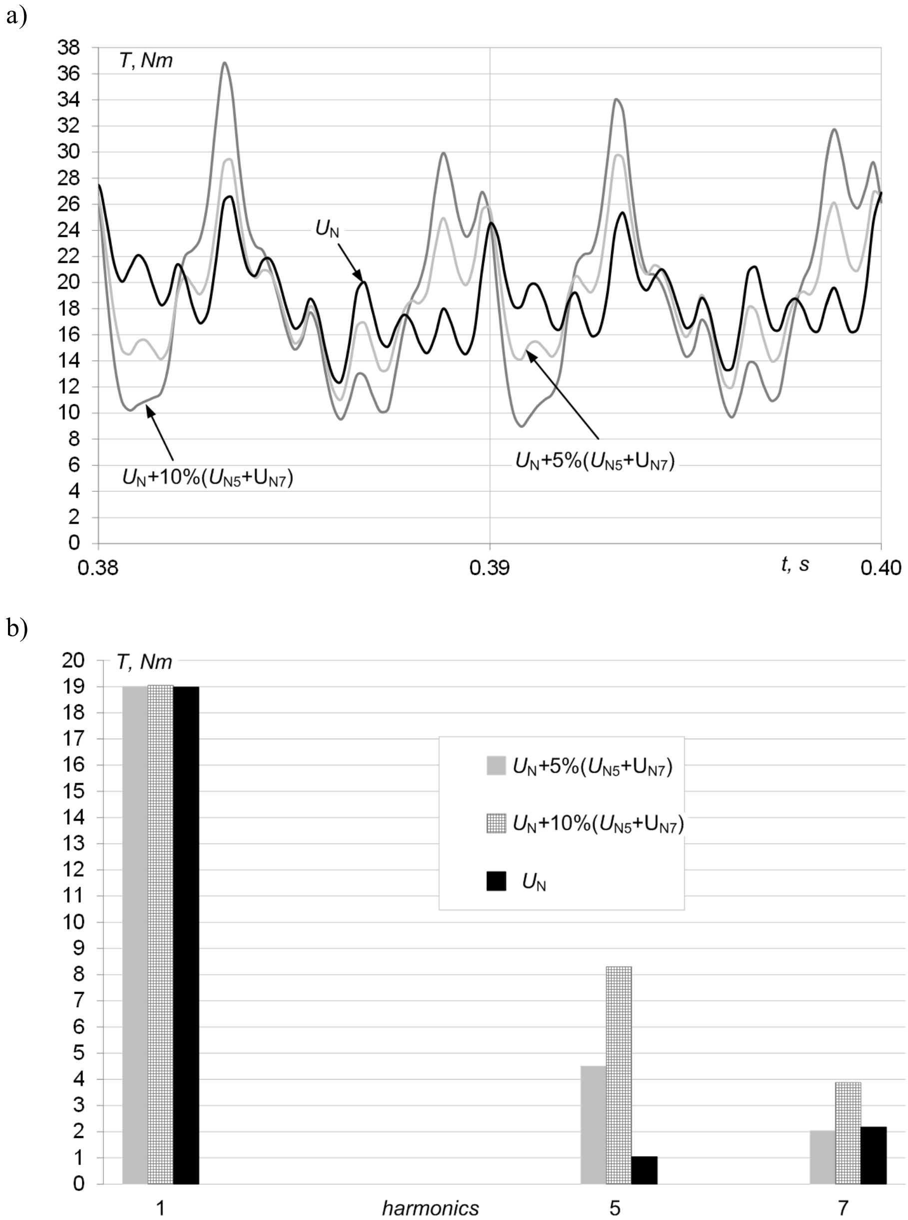

Fig. 6. Electromagnetic torque at 5% and 10% content of 5th and 7th harmonics: waveforms. (a), high harmonics analysis (b) – Comsol software

It can be seen that the amplitude of the calculated electromagnetic torque and phase current increases including with supply voltage distorted.

A comparison results obtained on the basis of in–house algorithm with the results obtained using Comsol package reveals close agreement. Unfortunately, comparisons of computing times are significant. The total numbers of discretized finite elements equal 37700 in in–house software and 43700 in Comsol, however, the total computational time using in–house software is typically about 40 minutes while Comsol package is 6 hours needed to achieve the same results.

5. CONCLUSION

On the basis of the simulation results the electromagnetic torque waveforms and phase current time curves of the permanent magnet synchronous motor for both in–house and commercial software were concluded.

The following conclusions can be drawn from the study:

- the increasing of oscillation of the electromagnetic torque is caused by the increasing high harmonics voltage,
- the increasing of high harmonics voltage cause deformation of phase currents, at constant load,
- the amplitude increasing of the electromagnetic torque and the deformation phase currents are caused by core saturation,
- the high harmonics supply voltage are reflected in the phase currents,
- the total time calculation in Comsol is more than 10 times larger than own.

REFERENCES

[1] Ogbuka C, Nwosu C, Agu M., Dynamic and steady state performance comparison of line–start permanent magnet synchronous motors with interior and surface rotor magnets, Archives of Electrical Engineering, Volume 65, Number 1, pp. 105–116, 2016.

[2] Młot A., Korkosz M., Łukaniszyn M., Iron loss and eddy–current loss analysis in a low–power BLDC motor with magnet segmentation, Archives of Electrical Engineering, Volume 61, Number 1, pp. 33–46, 2012.

[3] Gwoździewicz M., Zawilak J., Influence of the rotor construction on the single–phase line start permanent magnet synchronous motor performances, Electrical Review, Volume 87, Number 11, pp. 135–138, 2011.

[4] Wojciechowski R.M., Jędryczka C., Łukaszewicz P., Kapelski D., Analysis of high speed permanent magnet motor with powder material, COMPEL, Volume 31, Number 5, pp. 1528–1540, 2012.

[5] Fei. W., Luk K.P.C., Ma J., Shen J.X., Yang G., A high–performance line–start permanent magnet synchronous motor amended from a small industrial three–phase induction motor, IEEE Transactions on Magnetics, Volume 45, Number 1, pp. 4724–4727, 2009.

[6] Miller T.J.E., Popescu M., Cossar C., McGilp M.I., Strappazzon G., Trivillin N., Santarossa R., Line start permanent magnet motor: single–phase steady–state performance analysis, IEEE Transactions on Industry Applications, Volume 40, Number 2, pp. 516–525, 2004.
[7] Barański M., Szeląg W., Jędryczka C., Mikołajewicz J., Łukaszewicz P.: Analysis and tests of line start permanent magnet synchronous motor with u–shaped magnets rotor (in Polish), Electrical Review, Volume 89, Number 2b, pp. 107–111, 2013.
[8] Driesen J., Coupled electromagnetic–thermal problems in electrical energy transducers, Katholieke Universiteit Leuven, 2000.
[9] Demenko A., Finite element analysis of electromagnetic torque saturation harmonics in a squirrel cage machine, COMPEL – The international journal for computation and mathematics in electrical and electronic engineering, Volume 18, Number 4, pp. 619–628, 1999.
[10] Szeląg W., Analysis of analysis of transients and steady states and synthesis of permanent magnet synchronous motors, (in Polish) Wydawnictwo Politechniki Poznańskiej, Poznań, 1998.

(Received: 05. 02. 2017, revised: 16. 02. 2017)